Running Title: Role of DPPA5 in Human Pluripotent Stem Cells

DPPA5 Supports Pluripotency and Reprogramming by Regulating NANOG Turnover

Xu Qian[a,b], Jin Koo Kim[a,b], Wilbur Tong[a,b], Luis G. Villa-Diaz[a,b], Paul H. Krebsbach[a,b,c]

[a] *Department of Biologic and Materials Sciences, University of Michigan School of Dentistry, Ann Arbor, MI USA*
[b] *Biointerfaces Institute, University of Michigan, Ann Arbor, MI USA*
[c] *Department of Chemical Engineering, University of Michigan, Ann Arbor, MI USA*

Author contributions:
Xu Qian: Conception and design, collection and/or assembly of data, data analysis and interpretation, manuscript writing, final approval of manuscript
Jin Koo Kim: Collection and/or assembly of data, data analysis and interpretation, final approval of manuscript
Wilbur Tong: Collection and/or assembly of data, final approval of manuscript
Luis G. Villa-Diaz: Collection and/or assembly of data, data analysis and interpretation, final approval of manuscript
Paul H. Krebsbach: Conception and design, collection and/or assembly of data, data analysis and interpretation, manuscript writing, final approval of manuscript

Corresponding author: Paul H. Krebsbach, DDS, PhD
1011 N. University, Room K 1030, Ann Arbor, MI 48109-1078, USA.
Tel: +1 734 763 5280, Fax: +1 734 763 3453
E-mail Address: paulk@umich.edu (P.H. Krebsbach).

Funding:

This material is based upon work supported by the National Institutes of Health grant (R01DE016530-08 to PHK).

Key words: Embryonic stem cells, Induced pluripotent stem cells, DPPA5, NANOG, Cell reprogramming, Self-renewal, Pluripotency

ABSTRACT

Although a specific group of transcription factors such as OCT4, SOX2 and NANOG are known to play essential roles in pluripotent stem cell (PSC) self-renewal, pluripotency and reprogramming, other factors and the key signaling pathways regulating these important properties are not completely understood. Here, we demonstrate that the PSC marker Developmental Pluripotency Associated 5 (DPPA5) plays an important role in human PSC (hPSC) self-renewal and cell reprogramming in feeder-free conditions. Compared to hPSCs grown on mouse embryonic fibroblasts (MEFs), cells cultured on feeder-free substrates, such as Matrigel, Laminin-511, Vitronectin, or the synthetic polymer poly[2-(methacryloyloxy) ethyl dimethyl-(3-sulfopropyl) ammonium hydroxide] (PMEDSAH), had significantly higher DPPA5 gene expression and protein levels. Overexpression of DPPA5 in hPSCs increased NANOG protein levels via a post-transcriptional mechanism. Co-immunoprecipitation, protein stability assays and quantitative RT-PCR, demonstrated that DPPA5 directly interacted, stabilized and enhanced the function of NANOG in hPSCs. Additionally, DPPA5 increased the reprogramming efficiency of human somatic cells to induced pluripotent stem cells (hiPSCs). Our study provides new insight into the function of DPPA5 and NANOG regulation in hPSCs.

INTRODUCTION

Human pluripotent stem cells (hPSCs), which include embryonic stem cells (hESCs) derived from the inner cell mass of blastocyst-stage embryos, and induced pluripotent stem cells (hiPSCs) generated by reprogramming somatic cells through overexpression of key transcription factors [1-3], are promising resources for regenerative medicine. An improved understanding of these pluripotent cells may also provide insight into early human embryonic development because these cells are able differentiate into specialized cell types of all three germ layers and trophoectoderm. A key to unlocking this stem cell potential is by advanced understanding of the molecular mechanisms governing hPSC self-renewal and the network of factors that enable pluripotency. Although it is known that an assembly of transcription factors, including OCT4, SOX2 and NANOG, play important roles in hPSC self-renewal and pluripotency [4-7], the crucial signaling pathways and factors regulating these transcription factors is not completely understood.

The *Developmental Pluripotency Associated 5 (DPPA5)* gene, also designated *ESG1*, belongs to the *KHDC1/DPPA5/ECAT1/OOEP* gene family. These genes encode structurally related proteins characterized by an atypical RNA-binding K Homology (KH) domain and are specifically expressed in mammalian oocytes and ESCs [8]. Because of its high expression in pluripotent stem cells, DPPA5 has been used as an informative marker for pluripotency and stemness [9-14]. However, there is limited information regarding the function of DPPA5 in mouse or human ESCs [15].

The homeobox transcription factor NANOG has been proposed as a gatekeeper of pluripotency in hPSCs. Studies indicate that down-regulation of NANOG in hESCs induces differentiation [6], while overexpression of *NANOG* prevents neuroectoderm differentiation and blocks progression along endodermal and mesodermal lineages [16-18]. In methods to reprogram somatic cells into iPSCs, the addition of *NANOG* to the *OCT4*, *SOX2*, *KLF4*, and *C-MYC* (OSKM) reprograming cocktail enhances reprogramming kinetics [19]. Likewise, hiPSCs have been generated by the overexpression of *NANOG* in cooperation with the expression of *OCT4*, *SOX2*, and *LIN28* [3].

Here, we used DPPA5 as a PSC marker to investigate the mechanism by which synthetic polymer coatings such as poly[2-(methacryloyloxy) ethyl dimethyl-(3-sulfopropyl) ammonium hydroxide] (PMEDSAH) support hPSC self-renewal in feeder-free conditions [20, 21]. Our data revealed higher expression of DPPA5 in hPSCs cultured on PMEDSAH compared to irradiated mouse embryonic fibroblasts (MEFs), the most widely used culture condition [22]. This finding led us to raise the hypothesis that DPPA5 has a unique role in hPSCs self-renewal when cultured on synthetic substrates.

We first compared gene expression and protein levels of DPPA5 in hPSCs cultured on MEFs and several feeder-free conditions. In response to *DPPA5* overexpression,

NANOG protein levels were stabilized. Because of the central role of NANOG in hPSC pluripotency, we investigated the mechanism by which DPPA5 regulates NANOG and the effects of DPPA5 on NANOG target genes in hESCs. We also studied the function of DPPA5 in the derivation of hiPSCs and found *DPPA5* enhanced the reprogramming efficiency when combined with *OCT4*, *SOX2*, *KLF4*, and *C-MYC*.

MATERIALS AND METHODS

Cell culture substrates preparation

All cell culture was performed in designated incubators at 37°C in 5% CO_2 and high humidity. Irradiated MEFs (GlobalStem) were plated at a density of 2 X 10^4 cells/cm^2 on gelatin-coated tissue culture dishes. The fibroblast culture medium was composed of high-glucose DMEM (GIBCO), 10% fetal bovine serum (FBS; GIBCO), 1% nonessential amino acids (GIBCO), 1% GlutaMax (GIBCO) and 1% penicillin streptomycin (GIBCO).

The synthetic surface PMEDSAH was prepared as described previously [23]. Briefly, through ultraviolet ozone (UVO)-initiated free radical polymerization in a fume hood with connections for argon, a 500 ml reaction vessel was degassed by vacuum for 1 hour. When the reaction vessel was being evacuated, a monomer solution consisting of 0.25 M MEDSAH (Sigma-Aldrich) was dissolved in a mixture of deionized water and ethanol (4:1, v/v). The solution was degassed for 40 minutes with an argon purge.

After the reaction vessel and solvent were degassed, the monomer solution was transferred to a reaction vessel and heated to 68-70°C. While the reaction vessel was being heated, tissue culture polystyrene (TCPS) dishes (BD BioSciences) were activated by UVO treatment (Jetlight Inc.) for 40 minutes to create initiation sites on the surface. After activation, the dishes were transferred to a reaction vessel and the temperature was increased to 76-80°C. Surface-initiated polymerization occurred over a 2.5 hour time period under argon atmosphere at 76-80°C. Once the process was complete, TCPS dishes and control samples were removed from the reaction vessel and rinsed in a 1% saline (w/v) solution at 50°C.

Matrigel (BD BioSciences) was diluted to a concentration of 100 μg/ml in cold Dulbecco's modified Eagle's medium/F12 (DMEM/F12; GIBCO) and then applied to TCPS dishes or flasks (BD BioSciences). The coating was allowed to polymerize during 2 hours incubation at room temperature. Before plating cells, excess Matrigel-DMEM/F12 solution was aspirated and the dishes were washed with sterilized Dulbecco's phosphate buffered saline (D-PBS; GIBCO). Human Laminin-511 (Biolamina) was diluted to a concentration of 10 μg/ml in PBS (GIBCO). Vitronectin (R&D Systems) was diluted to 5 μg/ml in PBS (GIBCO). Coatings of Laminin or Vitronectin were applied to TCPS dishes following the manufacturer's protocols, respectively.

Cell culture of hPSCs

Unless otherwise specified, hESCs (H1, NIH registration # 0043 and H9, NIH

registration number # 0062 from WiCell Research Institute, Madison, WI; and CHB10, NIH registration number 0009 from Children's Hospital Corporation, Boston, MA) and hiPSCs derived in our lab [24] from human gingival fibroblasts and foreskin fibroblasts (hGF2-iPSCs, hGF4-iPSCs and hFF-iPSCs) were cultured on PMEDSAH, Matrigel, human Laminin-511, Vitronectin and MEFs with hPSC culture medium (human-cell-conditioned medium (HCCM, Global Stem) supplemented with 5 ng/ml of human recombinant basic fibroblast growth factor (bFGF; Invitrogen™) and 1% antibiotic-antimycotic (GIBCO). The hPSC culture medium was replaced every other day. Differentiated cells were mechanically removed with a sterile pulled-glass pipet under a stereomicroscope (LeicaMZ9.5, Leica Microsystems Inc.). Undifferentiated colonies were cut and passed as small cell clusters for three passages for each culture condition before analysis.

MEF-conditioned medium preparation and extracellular matrix (ECM) deposition

Twenty-four hours after plating irradiated MEFs at a density of 2 X 10^4 cells/cm^2 on gelatin-coated tissue culture dishes, fibroblast culture medium was replaced with hPSC culture medium, and collected the following day, and was labeled as MEF1-CM. Then, hPSC culture medium was replaced every other day and conditioned medium was collected again after 6 days (MEF7-CM). MEF-conditioned media were stored at −20°C before being used in hPSC culture. MEF-ECM deposits were prepared as described previously [22]. Briefly, irradiated MEFs were culture as described above and during the same period of time. At the time of isolating the ECM deposits, MEFs

were washed twice with phosphate buffered saline (PBS), and then lysed in buffer containing 0.5% (v/v) of Triton X-100/PBS and 0.035 ml of ammonium hydroxide solution (NH4OH) per 100 ml for 5 minutes at room temperature. Plates with ECM deposited were washed three times with PBS before being used in cell culture.

RNA isolation and quantitative RT-PCR

RNA was isolated and purified with the RNA easy Mini-Kit (Qiagen) following the manufacturer's protocol. RNA quality and concentration was measured with a Synergy NEO HTS Multi-Mode Microplate Reader (BioTek Instruments, Winooski, VT). Reverse transcription from 1 µg of total RNA into cDNA was done using SuperScript™ III First-Strand Synthesis SuperMix (Invitrogen™). Quantitative PCR was performed by TaqMan probes (Applied Biosystems) and TaqMan Universal PCR Master Mix (Applied Biosystems) on 7900 HT Fast Real Time PCR system (Applied Biosystems). Gene expression data was normalized to the expression levels of GAPDH, and calculated by the delta-delta *cT* expression level.

Western blot analysis

The following antibodies were used: OCT4 antibody (1:2,000; Cat. 4286, Cell Signaling), SOX2 antibody (1:1,000; Cat. 2748, Cell Signaling Technology), KLF4 antibody (1:1,000; Cat. 12173, Cell Signaling Technology), C-MYC antibody (1:1,000; Cat. 9402, Cell Signaling Technology), NANOG antibody (1:1,000; Cat. 3580, Cell Signaling Technology), DPPA5 antibody (2 µg/ml; Cat. MAB3984, R&D systems), DDK antibody (1: 2,000, Cat. TA50011, OriGene), α-tubulin antibody (1:3,000; Cat.

sc-8035, Santa Cruz Biotechnology) and β-actin antibody (1:1,000; Cat. 4970, Cell Signaling Technology). Whole cell lysates were prepared from cells, separated on 10% SDS-polyacrylamide gel, and transferred to polyvinylidene difluoride membranes. The membranes were incubated with 5% milk in TBST (w/v) for 0.5 hour and then incubated with primary antibodies overnight at 4°C. Blots were incubated with horseradish peroxidase-coupled secondary antibodies (Promega; R&D systems) for 1 hour, and protein expression was detected with SuperSignal West Pico Chemiluminescent Substrate or SuperSignal West Femto Chemiluminescent Substrate (Thermo Scientific). ImageJ software (http://rsb.nih.gov/ij) was used for quantification of Western blots.

Directed cell-lineage differentiation and embryoid body (EB) formation

EB formation was achieved by culturing clusters of hPSCs in suspension with DMEM (GIBCO) supplemented with 10% FBS for 10 days. Directed cell-lineage differentiation was performed on Matrigel coated dishes using the following protocols [25]. hPSCs were induced to differentiate in chemically defined medium (CDM) base consisting of DMEM/F12 (GIBCO) supplemented with 1X N2 (Invitrogen), 1X B27 (Invitrogen), 0.11 mM 2-mercaptoethanol, 1 mM nonessential amino acids, 2 mM L-glutamine, and 0.5 mg/ml BSA (fraction V; Sigma Aldrich). To induce definitive endoderm (pancreatic differentiation), 100 ng/ml human recombinant activin A (STEMGENT) was added to CDM and cells were then cultured in this condition for 6 days, followed by culture in CDM without activin A for another 9 days. For mesoderm (cardiomyocyte differentiation), cells were cultured in CDM supplemented with 50

ng/ml human recombinant BMP4 (STEMGENT) and 50 ng/ml human recombinant activin A (STEMGENT) for 4 days, then further cultured in CDM without activin A and BMP4 for an additional 10 days. For ectoderm (neuronal differentiation), 100 ng/ml human recombinant Noggin (STEMGENT) was added to the CDM and cells were cultured for 8 days. In addition, to test the impact of DPPA5 on hPSCs differentiation, neuroectoderm differentiation was induced as previously described [17]. Briefly, hESCs were grown in chemical defined medium with 10 μM SB431542 (Sigma-Aldrich) and 12 ng/ml bFGF (Invitrogen™) for 7 days.

Retrovirus production and transduction into cells

Retrovirus (10X) was produced with the plasmids *pMXs-hOCT3/4*, *pMXs-hSOX2*, *pMXs-hKLF4*, *pMXs-hC-MYC*, *pMXs-DPPA5* and *pMXs-GW* (as control) (Addgene plasmids #: 17217, 17218, 17219, 17220, 13352 and 18656, respectively); by the University of Michigan Vector Core using standard protocols.

***DPPA5* overexpression**

Single hPSCs (2 X 10^4) were plated on a Matrigel-coated 60 mm TCPS dishes in hPSC culture medium supplemented with 10 μM of Rho-associated coiled coil forming protein serine/threonine kinase (ROCK) inhibitor (Sigma-Aldrich) and infected with *DPPA5* retroviruses. Fibroblasts (1.5 X 10^5) were plated on a 35 mm TCPS dishes in fibroblast culture medium and infected by 1X *DPPA5* retroviruses plus polybrene (10 μg/ml; Sigma-Aldrich) when cell confluence reached about 60%. In addition, fibroblasts were also transfected in a 35 mm TCPS dish with 2 μg

pCMV6-Entry plasmid containing *DPPA5* human cDNA ORF Clone (Cat. RC222509, OriGene) using FuGENE 6 transfection reagent (Promega). The construct pCMV6-Entry (OriGene) was used as a control. DDK-tagged DPPA5 plasmid (Cat. RC222509, OriGene) was transfected into hESCs using a modified-reversed transfection protocol [26]. Briefly, 2 µg of DDK-tagged DPP5 plasmid-FuGENE 6 complex were mixed with Matrigel during the 2 h polymerization period. Single hESCs were then seeded on Matrigel-plasmid coated dishes, and cell culture medium was replaced the following day.

Co-immunoprecipitation

Immunoprecipitation (IP) was performed using the ImmunoCruz™ IP/WB Optima C System (Santa Cruz Biotechnology) following the manufacturer's protocol. Briefly, hESCs protein extracts were prepared in CHAPS lysis and IP buffer (FIVEphoton Biochemicals) with protease inhibitor (FIVEphoton Biochemicals) and phosphatase inhibitor (FIVEphoton Biochemicals). hESC lysate (700 µg of total protein) was precleared with Preclearing Matrix C-mouse (Santa Cruz Biotechnology) for 1.5 hours at 4°C on a rotator. Meanwhile, NANOG antibody (Cat. ab62734, Abcam), DDK antibody (Cat. TA50011, OriGene), OCT4 antibody (Cat. 4286, Cell Signaling), SOX2 antibody (Cat. 2748, Cell Signaling), normal mouse IgG (Santa Cruz Biotechnology) or normal rabbit IgG (Santa Cruz Biotechnology) were mixed and incubated to form IP antibody-IP matrix complex and the control-IP matrix complex, respectively. After 1 hour of incubation at 4°C on a rotator, IP antibody-IP matrix complex was washed with PBS (GIBCO). The supernatant was discarded after centrifugation. The precleared

hPSCs lysate supernatant was transferred to the pelleted IP antibody-IP matrix complex and incubated at 4°C on a rotator for 4 hours. After incubation and centrifugation, pelleted matrix was washed with PBS and Western blot analysis was performed to detect the interaction between DPPA5 and NANOG, OCT4 or SOX2. Whole hPSCs lysate was used as input.

Protein stability assay

hPSCs were infected with DPPA5 or control (pMXs-GW) retroviruses. After 72 hours, cycloheximide (CHX; Sigma-Aldrich) was added to the culture medium at a concentration of 45 μg/ml. CHX treatment lasted until cells were subsequently harvested at different time points (0.5 hours, 1 hours, 1.5 hours after CHX addition). Equal amounts of protein were loaded from each treated sample and analyzed by Western blot assays.

Immunofluorescence staining

Cells were fixed in 4% paraformaldehyde for 30 minutes at room temperature and then permeabilized with 0.1% Triton X-100 for 10 minutes. Primary antibodies against DPPA5 (Cat. MAB3984, R&D systems), NANOG (Cat. ab62734, Abcam), SSEA4 (Cat. sc-21704, Santa Cruz Biotechnology), OCT4 (Cat. sc-8629, Santa Cruz Biotechnology), SOX2 (ab5603, Millipore), TRA-1-81 (Cat. mab4381, Millipore), SSEA3 (Cat. mab4303, Millipore), TRA-1-60 (Cat. sc-21705, Santa Cruz Biotechnology) were diluted in 1% normal serum (v/v) and incubated overnight at 4°C and detected with respective secondary antibodies. Sample images were captured

using a Nikon TE2000-S inverted microscope with a Nikon DS-Ri1 camera, or using Nikon confocal microscope system A1^{+}.

Derivation of hiPSCs and quantification of reprogramming efficiency

For iPSC reprogramming, 1.5 X 10^5 human gingival fibroblasts were plated on 35 mm TCPS dishes in fibroblast culture medium. When cell confluence reached about 60%, cells were infected by retroviruses (*KLF4, C-MYC, OCT4* and *SOX2; KMOS*) using the method described above. In experimental groups, fibroblasts were also infected with retroviruses carrying *DPPA5* on day 0, day 6, day 9 and day 12, respectively. Three days after KMOS infection, cells were trypsinized and passed to Matrigel-coated or MEF-plated flasks (75 cm^2). At that time, the fibroblast culture medium was replaced by hPSC culture medium supplemented with 10 μM of ROCK inhibitor (Sigma-Aldrich). The hPSC culture medium with ROCK inhibitor was refreshed every day until day 23, when cells were either analyzed by alkaline phosphatase activity or submitted for flow cytometry analysis. Alkaline phosphatase activity and colony morphology (well defined borders and high nuclei/cytoplasmic ratio) were used to identify reprogrammed hiPSC colonies (Fig. S3C-D). The number of hiPSC colonies in control and experimental groups were quantified and used to calculate the reprogramming efficiency as follows: the number of hiPSC colonies in each group was divided by 1.5 X 10^5, which was the original number of fibroblasts plated for each group before reprogramming.

Alkaline phosphatase staining

Alkaline phosphatase staining was done with the Alkaline Phosphatase Staining Kit (STEMGENT). Cells were fixed with Fixing Solution for 2-5 minutes, then rinsed and incubated in AP Substrate Solution in the dark at room temperature for 15 minutes. Cells were rinsed and covered with 1 X PBS to prevent drying before quantitative analysis.

Flow cytometry analysis

Cells were washed with PBS and harvest by incubation in 0.25% trypsin-EDTA (GIBCO). After trypsinization, the cells were incubated first with human IgG to block nonspecific binding and then with SSEA-4 phycoerythrin (PE)-conjugated antibody (Cat. FAB1435p, R&D systems) or mouse anti-human TRA-1-60 PE-conjugated antibody (Cat. 560193, BD Pharmingen) and then analyzed by flow cytometry. Analysis was carried out with MoFlo® Astrios™ (Beckman Coulter) using standard procedures. Background fluorescence and autofluorescence were determined using cells incubated with Mouse IgG1 PE isotype control (Cat. 1c002p, R&D systems).

Statistical analysis

At least three independent replicates of each experiment were performed. Two data sets were compared using the student t-test function in Excel (Microsoft, Seattle, WA) to calculate p-values. Multiple data sets were compared using one-way ANOVA analysis followed by the Tukey's post-hoc test to calculate p-values. Level of statistical significance was set at $p < 0.05$.

RESULTS

DPPA5 expression in hPSCs is higher when cultured on feeder-free substrates than on MEFs

To investigate the mechanism by which synthetic substrates such as PMEDSAH support hPSC self-renewal in feeder-free conditions, we compared the expression of pluripotency-related genes in H9 hESCs cultured on PMEDSAH versus MEFs after three consecutive passages. Quantitative RT-PCR analysis demonstrated that *DPPA5* gene expression levels were significantly higher in hESCs cultured on PMEDSAH compared to on MEFs, while the expression of other pluripotency-related factors such as *OCT4*, *SOX2*, *KLF4*, *C-MYC* and *NANOG* was not significantly changed (Fig. 1A). Similar results were obtained with the CHB10 hESC line and three independent hiPSC lines (Fig. 1B). Western blot analysis demonstrated that protein levels of DPPA5 and NANOG were higher in hPSCs cultured on PMEDSAH compared to MEFs, while other pluripotency-related factors showed no significant differences (Fig. 1C). The mRNA expression of *DPPA5* in hPSCs was then compared to cells cultured on MEFs and other feeder-free conditions (Matrigel, Laminin-511 and Vitronectin). Quantitative RT-PCR analysis demonstrated higher gene expression of *DPPA5* in hPSCs grown on feeder-free substrates compared to cells cultured on MEFs, while no significant mRNA expression differences were observed among hESCs cultured in these feeder-free conditions (Fig. 1D).

Previously, we demonstrated that both the extracellular matrix (ECM) and soluble factors secreted by MEFs significantly impact the self-renewal of hESCs [22]. Therefore, we hypothesized that the ECM and soluble factors secreted by MEFs may inhibit *DPPA5* expression in hPSCs, compared to feeder-free conditions. MEF-conditioned medium and ECM deposits were prepared on TCPS dishes as described in the Materials and Methods section, and used to culture hESCs for three passages. The combination of PMEDSAH and HCCM was set as the control culture condition. In addition, cells were cultured on PMEDSAH plus day 1 or day 7 MEF-conditioned medium (CM), and day 1 or day 7 MEF-ECM plus HCCM. The mRNA expression of *OCT4* was used as an indicator of the undifferentiated state of hESCs. Quantitative RT-PCR analysis demonstrated that, compared to the control condition, hPSCs expressed significantly lower levels of *DPPA5* in PMEDSAH with day 7 MEF-conditioned medium (Fig. 2A), indicating that soluble factors secreted by MEFs inhibit *DPPA5* expression. Similarly, compared to the control condition, the expression of *DPPA5* was significantly lower in hPSCs cultured on MEF-ECM plus HCCM (Fig. 2B), indicating that the ECM deposited by MEFs also inhibits *DPPA5* expression in hPSCs. Taken together, these data suggested that soluble factors and ECM deposited by irradiated MEFs inhibit DPPA5 gene expression in hPSCs.

We analyzed *DPPA5* gene expression levels in hPSCs and their differentiated derivative cells. Quantitative RT-PCR demonstrated that *DPPA5* expression levels were significantly upregulated in hiPSCs compared to their corresponding parental

fibroblasts (Fig. 3A). Conversely, when compared to undifferentiated hESCs, *DPPA5* expression levels significantly decreased after embryoid body (EB) formation (Fig. 3B) and in cells induced to endodermal, mesodermal and ectodermal lineages (Fig. 3C). Cell lineage differentiation and EB formation was confirmed by increasing expression of factors representative of each germ layer (Fig. S1, Table S1).

Immunocytochemistry analysis demonstrated that DPPA5 and NANOG protein were observed in undifferentiated hESCs and decreased in differentiated cells (Fig. S2A-B). Our finding that DPPA5 expression was higher in undifferentiated hPSCs compared to differentiated cells is consistent with other studies that used DPPA5 as a PSC marker [9, 12-14, 27-30]. This specific expression pattern suggested that DPPA5 might play an important role in hPSC self-renewal and pluripotency.

DPPA5 regulates NANOG protein levels

The higher expression of DPPA5 in hPSCs cultured under feeder-free conditions compared to MEFs provoked our interest in elucidating the function of DPPA5. Overexpression of *DPPA5* in fibroblasts did not significantly affect gene expression of *OCT4, SOX2, KLF4, C-MYC* and *NANOG* (Fig. 4A). However, in fibroblasts with overexpressed DPPA5, in addition to detecting a significant increase in DPPA5 protein levels, we also observed an increase in NANOG protein levels via Western blot analysis (Fig. 4B). No change in protein levels was detected for other pluripotency-related factors. The same pattern was observed when *DPPA5* was overexpressed in hESCs. NANOG protein levels dramatically increased without

significant changes in gene expression (Fig. 4C-D). These data indicated that DPPA5 functions as a positive regulator of NANOG protein at a post-transcriptional level.

DPPA5 protein interacts with and stabilizes NANOG protein

Next, we investigated the extent to which DPPA5 may affect NANOG protein levels in hPSCs. Immunofluorescence staining and confocal microscopy analysis illustrated that DPPA5 was localized in both the cytoplasm and nucleus of hESCs. In addition, DPPA5 co-localized with NANOG in the nucleus (Fig. 5A), indicating a potential interaction between these two proteins.

Co-immunoprecipitation was performed to determine the interaction between DPPA5 and NANOG in hESCs. Western blot analysis demonstrated that NANOG was successfully immunoprecipitated with a NANOG IP antibody-IP matrix complex (Fig. 5B). Concurrent with this finding, DPPA5 was strongly co-precipitated with NANOG (Fig. 5B). Immunoprecipitation of DPPA5 was achieved by pulling-down DDK protein from hESCs transfected with a DDK-tagged DPPA5 plasmid. NANOG was co-precipitated with DDK–tagged DPPA5 (Fig. 5C). These data indicated the interaction between DPPA5 and NANOG protein. No protein was co-precipitated by the normal mouse IgG-IP matrix complex, suggesting nonspecific binding did not play a role in these experiments. Furthermore, DPPA5 was not co-precipitated with OCT4 or SOX2 (Fig. S2C-D), which suggested the specificity of interaction between DPPA5 and NANOG proteins. Protein stability assays were then performed to determine the extent to which DPPA5 inhibits NANOG protein degradation in hESCs. Western blot

analysis demonstrated that the degradation of NANOG was significantly delayed by *DPPA5* overexpression in the presence of cycloheximide (Fig. 5D). Taken together, these data indicated that DPPA5 interacts with NANOG and stabilizes NANOG in hPSCs.

DPPA5 enhances the function of NANOG

NANOG increases the transcription of *SALL4*, and represses the transcription of *GATA6* and *SOCS3* through binding to their proximal gene promoters [31-35]. To study the extent to which DPPA5 enhances the function of NANOG in hPSCs, we examined the expression of NANOG target genes (*SALL4*, *GATA6* and *SOCS3)* in response to *DPPA5* overexpression. The overexpression of DPPA5 in hESCs is shown in Fig. 4C-D. We found that gene expression of *SALL4* was increased, while *GATA6* and *SOCS3* were repressed after *DPPA5* overexpression (Fig. 6A). This evidence suggested that DPPA5 not only increased NANOG protein levels through post-translational stabilization, but also facilitated the function of NANOG on its target genes.

To test the impact of DPPA5 on NANOG in hESC differentiation, we induced hPSC neuroectoderm differentiation in control and DPPA5 overexpressed hESCs with the knowledge that overexpression of *NANOG* blocks neuroectoderm differentiation [17]. We observed that after induced neuroectoderm differentiation in hESCs, the expression levels of pluripotency markers such as *OCT4* and *SOX2* were decreased, while neuroectordern markers *SOX1* and *NEUROD1* were increased in both control

and DPPA5 overexpressed cells (Fig. 6B). Interestingly, in neuroectoderm differentiated cells, the expression levels of *SOX1* and *NEUROD1* were lower in DPPA5 overexpressed cells compared to controls (Fig. 6B). Taken together, these data indicated that DPPA5 promotes the function of NANOG .

DPPA5 increases hiPSC-reprogramming efficiency

Because of the stabilizing action of DPPA5 on NANOG in hESCs and the critical role of NANOG in hPSCs self-renewal and in the generation of hiPSCs [3, 19], we investigated whether DPPA5 could have a positive effect during reprograming of fibroblasts into hiPSCs (Fig. S3A-B). *DPPA5* was added to the *KLF4*, *C-MYC, OCT4*, *SOX2 (KMOS)* reprogramming cocktail to determine its effect on reprogramming of fibroblast into hiPSCs. Retroviruses encoding the *KMOS* cocktail were used to infect fibroblasts in both control and experimental groups on day 0. Experimental groups were additionally infected with retroviruses encoding *DPPA5* on day 0, day 6, day 9 and day 12 (experimental group-d0+D, d6+D, d9+D and d12+D, respectively). On day 23, hiPSC colonies were classified as successfully reprogrammed or as pre-iPSCs by the following criteria: reprogrammed colonies should have positive alkaline phosphatase staining and well-defined borders and cells should have a high nucleus:cytoplasm ratio (Fig. S3C). Pre-iPSCs were identified by undefined borders even if exhibiting alkaline phosphatase activity (Fig. S3D). We found that overexpression of *DPPA5* on day 6, day 9, day 12, but not day 0, significantly ($p<0.05$) enhanced the generation of hiPSC colonies compared to the control group, (Fig. 7; Table S2). The reprogramming efficiency was increased from 0.023% to 0.076%

between the control group and the d9+D group. In addition, flow cytometry analysis at day 23, confirmed that the percent of both TRA-1-60^{+} cells and SSEA4^{+} cells was higher in d6+D groups compared to controls without DPPA5 and in cells reprogrammed in feeder free conditions compared to cells on feeder cells (Fig. S4).

The derived hiPSCs from both control and d6+D groups were characterized by immunostaining with markers for pluripotency (Fig. S3E-F) and analysis of representative genes of the three germ layers after EB formation (Tables S3-4). Taken together, our results indicate that DPPA5 had an additive effect to the reprogramming cocktail of OCT4, SOX2, KLF4, and C-MYC by increasing hiPSC-reprogramming efficiency.

DISCUSSION

The potential for successful therapeutic application of hPSCs and their derivatives will depend, in part, on the ability to develop clinically compliant strategies for large-scale production of therapeutically relevant cells [36-38]. The large-scale expansion of hPSCs has been limited by xenogeneic components and poorly defined culture conditions that utilize feeder cells and other animal-based products to support hESC self-renewal [1, 39, 40]. To overcome these limitations, the use of feeder-free conditions with human recombinant proteins like Laminin and Vitronectin have been tested for long-term maintenance of hESCs [41, 42]. The combination of these xenogeneic-free substrates and chemically defined media such as mTesR, E-8 and

X-VIVO10 [41, 43-45] represents significant progress in the development of hPSC culture systems.

Moreover, synthetic substrates such as PMEDSAH [20, 21] have demonstrated great potential for large-scale propagation of hESCs [46]. Our data suggest that in MEF conditions, the synthesis of soluble factors and the deposition of undefined ECM proteins inhibit DPPA5 expression in hPSCs compared to feeder-free culture conditions. These findings are consistent with our previous report that showed the capacity of γ-irradiated MEFs to support hESC self-renewal is compromised over time due to changes in the secretion of soluble factors and ECM [22]. These data support the trend in the evolution of hPSC culture from feeder-cell dependence and ill-defined conditions, to feeder-free and defined microenvironments [47].

Pluripotency and self-renewal are maintained in PSCs by a network of interacting transcription factors, influenced by specific signaling pathways [48], and these interactions may be different depending on the *in vitro* culture conditions. Our data identifies DPPA5 as a new component in this regulatory network of pluripotency that is differentially expressed depending on the culture conditions. DPPA5 is highly expressed in feeder-free conditions (PMEDSAH, Matrigel, Laminin-511 and Vitronectin) compared to feeder-dependent conditions (MEFs), suggesting that DPPA5 may play a more important role in hPSC maintenance under feeder-free conditions. Our findings that the molecular mechanisms supporting hPSC

pluripotency are different depending on the culture conditions, as well as species differences between human and mouse ESCs, may explain discrepancies with a previous finding of no significant impact on mouse ESC self-renewal when *DPPA5* was knocked and cells were cultured on MEFs [11].

The identification of a functionally significant role for DPPA5 in hPSC self-renewal may contribute to a better understanding of how feeder-free conditions support hPSC self-renewal. This is especially important since the use of hPSCs in regenerative medicine will likely be dependent on the use of xenogenic and feeder-free conditions. Our data indicate that in hPSCs, DPPA5 regulates NANOG protein stability and enhances its function on target genes, which may result in pro-pluripotency conditions that better support self-renewal. This new finding in the regulation of NANOG by DPPA5 is important because of the central role that this transcription factor plays in PSC regulatory networks. NANOG is a homeodomain protein that regulates the transcriptional levels of other genes, such as *SALL4*, *GATA6* and *SOCS3* [31-35, 49]. Previous findings demonstrating that down-regulation of NANOG in hESCs induces differentiation [6], while its overexpression prevents differentiation [16-18], suggest that sufficient levels of NANOG are critical for hPSC self-renewal. Our study suggests that DPPA5 plays an important role in supporting hPSC self-renewal by facilitating the protein levels of NANOG, a master transcriptional regulator for hPSC pluripotency. DPPA5 inhibits hPSC differentiation by stabilizing NANOG protein levels and enhancing the up-regulatory effects of NANOG on *SALL4*, a transcription factor

required for ESC pluripotency, and down-regulatory effects of NANOG on *GATA6 and SOCS3*, well known NANOG target genes that function in early stages of differentiation [35, 50, 51].

Another novel and potentially important finding is the mechanism by which DPPA5 facilitates NANOG protein levels. Previous studies reported transcriptional regulation of *NANOG* by other pluripotency-related factors such as OCT4, SOX2 and KLF4 [52, 53]. Meanwhile, DPPA5 has been reported to be an RNA binding protein because it contains a KH domain [8]. Interestingly, we found that NANOG protein levels increased after *DPPA5* overexpression without significant changes at *NANOG* mRNA levels. We also found that both mRNA and protein levels of other key pluripotent-related transcription factors (OCT4, SOX2 and KLF4) remained unchanged after *DPPA5* overexpression. These findings led us to raise the hypothesis that DPPA5 directly interacts with and stabilizes NANOG proteins, which is supported by the co-immunoprecipitation and protein stability results. In support of these findings, a previous study showed that DPPA5 does not bind to, and regulate *NANOG* RNA after an immunoprecipitation-microarray screening [15]. In addition, our findings of the post-translational regulation of NANOG are consistent with other studies showing that, like other pluripotency-related transcription factors such as OCT4, KLF4 and C-MYC, NANOG is also an unstable protein with a relatively short half-life in hPSCs. These transcription factors are degraded through ubiquitin-dependent proteolysis [54-58], while proteasome inhibitors are able to block

NANOG protein degradation in hPSCs and extend its half-life [59]. Our finding that DPPA5 interacts with and stabilizes NANOG provide an additional mode of regulation of NANOG in hPSCs, suggesting that in addition to the broadly investigated transcriptional regulation of pluripotency-related transcription factors, post-translational regulation also plays a role in the hPSC pluripotency regulatory network. We also observed that DPPA5 protein, like NANOG and other pluripotency-related factors, is degraded in a rapid manner in hPSCs (Fig. 5D). Thus, this regulatory model not only supports the hypothesis that DPPA5 is able to regulate NANOG, but also furthers our understanding of the molecular mechanisms that define hPSC pluripotency on synthetic substrates.

Human iPSCs reprogrammed from adult somatic cells by the process of induced pluripotency holds great potential for disease modeling, drug screening and cell replacement therapy [60]. We found that the addition of *DPPA5* at 6, 9 or 12 days after initial *OSKM* cocktail treatment increased the generation of hiPSCs by 3-fold compared to controls, or when *DPPA5* is over-expressed with *OSKM* on day 0. This observation suggests that *DPPA5* may have an optimal window for being overexpressed in cells to efficiently promote iPSC-reprogramming and may be related to the timing of NANOG expression in the reprogramming process [61]. The central role of NANOG in reprogramming of somatic cells into iPSCs [3, 19, 62, 63], combined with our finding that DPPA5 regulates NANOG protein levels, suggests that DPPA5 may promote hiPSC-generation efficiency by enhancing NANOG stability and

its function. This new finding is also consistent with a recent study showing the benefit of sequential introduction of reprogramming factors [64] in which a sequential epithelial-to-mesenchymal transition followed by mesenchymal-to-epithelial transition (EMT-MET) mechanism optimizes reprogramming. Interestingly, we observed a significant ($p<0.05$) increase in the number of cells expressing the pluripotent markers TRA-1-60 and SSEA4 in cells that were infected with DPPA5 at day 6 compared to controls when MEFs were used as a substrate compared to the Matrigel group. This is consistent with our conclusion that factors secreted by MEFs negatively affected the expression and function of DPPA5 and NANOG, and may affect the reprogramming efficiency of hiPSCs as well. Taken together, our data suggest an additive effect of DPPA5 in hiPSC generation, extends our knowledge of iPSC reprogramming, and may further advance current reprogramming protocols.

CONCLUSION

We provide new molecular insight into the function of the pluripotent stem cell marker DPPA5 in hPSCs. We established a role for DPPA5 in hPSCs and identified new functions of DPPA5 in hPSC biology, NANOG regulation and iPSC reprogramming. *In vitro* culture conditions influence the expression of DPPA5 in hPSCs. The ECM deposited by irradiated MEFs, as well as secreted soluble factors, inhibit the expression of DPPA5 in hPSCs, while its expression and function is permissive under feeder-free conditions. DPPA5 stabilizes NANOG and enhances the function of NANOG, a key transcription factor for hPSC pluripotency, which results in support of hPSC self-renewal. Finally, *DPPA5* increases the reprogramming efficiency of

somatic cells into human iPSCs when transduced with *OCT4, SOX2, KLF4* and *C-MYC*. In conclusion, DPPA5 plays an important role in supporting hPSC self-renewal and reprogramming on synthetic substrates. Our findings advance our knowledge of hPSC biology and offer improvements to current protocols in hPSC maintenance and reprogramming, which may contribute to the future application of these cells in regenerative medicine.

ACKNOWLEDGMENTS

The authors thank Dr. Joerg Lahann and his lab for their assistance in preparing PMEDSAH plates, Dr. Shinya Yamanaka for the gift of the plasmids (Addgene plasmid #: 17217, 17218, 17219, 17220, 13352 and 18656), and the National Institutes of Health (R01DE016530-08 to PHK) for support.

DISCLOSURE OF POTENTIAL CONFLICTS OF INTEREST

There are no potential conflicts of interest related to individual authors' commitments and any project supports.

REFERENCES

1 Thomson JA, Itskovitz-Eldor J, Shapiro SS et al. Embryonic stem cell lines derived from human blastocysts. Science 1998;282:1145-1147.

2 Takahashi K, Tanabe K, Ohnuki M et al. Induction of pluripotent stem cells from

adult human fibroblasts by defined factors. Cell 2007;131:861-872.

3 Yu J, Vodyanik MA, Smuga-Otto K et al. Induced pluripotent stem cell lines derived from human somatic cells. Science 2007;318:1917-1920.

4 Hay DC, Sutherland L, Clark J et al. Oct-4 knockdown induces similar patterns of endoderm and trophoblast differentiation markers in human and mouse embryonic stem cells. Stem Cells 2004;22:225-235.

5 Boyer LA, Lee TI, Cole MF et al. Core transcriptional regulatory circuitry in human embryonic stem cells. Cell 2005;122:947-956.

6 Hyslop L, Stojkovic M, Armstrong L et al. Downregulation of NANOG induces differentiation of human embryonic stem cells to extraembryonic lineages. Stem Cells 2005;23:1035-1043.

7 Fong H, Hohenstein KA, Donovan PJ. Regulation of self-renewal and pluripotency by Sox2 in human embryonic stem cells. Stem Cells 2008;26:1931-1938.

8 Pierre A, Gautier M, Callebaut I et al. Atypical structure and phylogenomic evolution of the new eutherian oocyte- and embryo-expressed KHDC1/DPPA5/ECAT1/OOEP gene family. Genomics 2007;90:583-594.

9 Kim SK, Suh MR, Yoon HS et al. Identification of developmental pluripotency associated 5 expression in human pluripotent stem cells. Stem Cells 2005;23:458-462.

10 Western P, Maldonado-Saldivia J, van den Bergen J et al. Analysis of Esg1 expression in pluripotent cells and the germline reveals similarities with Oct4 and Sox2 and differences between human pluripotent cell lines. Stem Cells

2005;23:1436-1442.

11 Amano H, Itakura K, Maruyama M et al. Identification and targeted disruption of the mouse gene encoding ESG1 (PH34/ECAT2/DPPA5). BMC Dev Biol 2006;6:11.

12 Aoki T, Ohnishi H, Oda Y et al. Generation of induced pluripotent stem cells from human adipose-derived stem cells without c-MYC. Tissue Eng Part A 2010;16:2197-2206.

13 Mamidi MK, Pal R, Mori NA et al. Co-culture of mesenchymal-like stromal cells derived from human foreskin permits long term propagation and differentiation of human embryonic stem cells. J Cell Biochem 2011;112:1353-1363.

14 Zhang Y, Wei C, Zhang P et al. Efficient reprogramming of naive-like induced pluripotent stem cells from porcine adipose-derived stem cells with a feeder-independent and serum-free system. PLoS One 2014;9:e85089.

15 Tanaka TS, Lopez de Silanes I, Sharova LV et al. Esg1, expressed exclusively in preimplantation embryos, germline, and embryonic stem cells, is a putative RNA-binding protein with broad RNA targets. Dev Growth Differ 2006;48:381-390.

16 Wang Z, Oron E, Nelson B et al. Distinct lineage specification roles for NANOG, OCT4, and SOX2 in human embryonic stem cells. Cell Stem Cell 2012;10:440-454.

17 Vallier L, Mendjan S, Brown S et al. Activin/Nodal signalling maintains pluripotency by controlling Nanog expression. Development 2009;136:1339-1349.

18 Suzuki A, Raya A, Kawakami Y et al. Nanog binds to Smad1 and blocks bone morphogenetic protein-induced differentiation of embryonic stem cells. Proc Natl Acad Sci U S A 2006;103:10294-10299.

19 Hanna J, Saha K, Pando B et al. Direct cell reprogramming is a stochastic process amenable to acceleration. Nature 2009;462:595-601.

20 Villa-Diaz LG, Nandivada H, Ding J et al. Synthetic polymer coatings for long-term growth of human embryonic stem cells. Nat Biotechnol 2010;28:581-583.

21 Nandivada H, Villa-Diaz LG, O'Shea KS et al. Fabrication of synthetic polymer coatings and their use in feeder-free culture of human embryonic stem cells. Nat Protoc 2011;6:1037-1043.

22 Villa-Diaz LG, Pacut C, Slawny NA et al. Analysis of the factors that limit the ability of feeder cells to maintain the undifferentiated state of human embryonic stem cells. Stem Cells Dev 2009;18:641-651.

23 Qian X, Villa-Diaz LG, Kumar R et al. Enhancement of the propagation of human embryonic stem cells by modifications in the gel architecture of PMEDSAH polymer coatings. Biomaterials 2014;35:9581-9590.

24. Villa-Diaz LG, Kim JK, Lahann J et al. Derivation and long-term culture of transgene-free human induced pluripotent stem cells on synthetic substrates. Stem Cells Transl Med 2014;3:1410-1417.

25. Yao S, Chen S, Clark J et al. Long-term self-renewal and directed differentiation of human embryonic stem cells in chemically defined conditions. Proc Natl Acad Sci U S A 2006;103:6907-6912.

26. Villa-Diaz LG, Garcia-Perez JL, Krebsbach PH. Enhanced transfection efficiency of human embryonic stem cells by the incorporation of DNA liposomes in extracellular matrix. Stem Cells Dev 2010;19:1949-1957.

27. Adjaye J, Huntriss J, Herwig R et al. Primary differentiation in the human blastocyst: comparative molecular portraits of inner cell mass and trophectoderm cells. Stem Cells 2005;23:1514-1525.

28. Xue F, Ma Y, Chen YE et al. Recombinant rabbit leukemia inhibitory factor and rabbit embryonic fibroblasts support the derivation and maintenance of rabbit embryonic stem cells. Cell Reprogram 2012;14:364-376.

29. Kues WA, Herrmann D, Barg-Kues B et al. Derivation and characterization of sleeping beauty transposon-mediated porcine induced pluripotent stem cells. Stem Cells Dev 2013;22:124-135.

30. Koh S, Thomas R, Tsai S et al. Growth requirements and chromosomal instability of induced pluripotent stem cells generated from adult canine fibroblasts. Stem Cells Dev 2013;22:951-963.

31. Frankenberg S, Gerbe F, Bessonnard S et al. Primitive endoderm differentiates via a three-step mechanism involving Nanog and RTK signaling. Dev Cell 2011;21:1005-1013.

32. Singh AM, Hamazaki T, Hankowski KE et al. A heterogeneous expression pattern for Nanog in embryonic stem cells. Stem Cells 2007;25:2534-2542.

33. Marson A, Levine SS, Cole MF et al. Connecting microRNA genes to the core transcriptional regulatory circuitry of embryonic stem cells. Cell 2008;134:521-533.

34. Stuart HT, van Oosten AL, Radzisheuskaya A et al. NANOG amplifies STAT3 activation and they synergistically induce the naive pluripotent program. Curr Biol 2014;24:340-346.

35. Lim CY, Tam W, Zhang et al. Sall4 regulates distinct transcription circuitries in different blastocyst-derived stem cell Lineages. Cell Stem Cell 2008; 3:543-54.

36. McCall MD, Toso C, Baetge EE et al. Are stem cells a cure for diabetes? Clin Sci 2010;118:87-97.

37 Dominguez-Bendala J, Inverardi L, Ricordi C. Stem cell-derived islet cells for transplantation. Curr Opin Organ Transplant 2011;16:76-82.

38. Laflamme MA, Chen KY, Naumova AV et al. Cardiomyocytes derived from human embryonic stem cells in pro-survival factors enhance function of infarcted rat hearts. Nat Biotechnol 2007;25:1015-1024.

39. Richards M, Tan S, Fong CY et al. Comparative evaluation of various human feeders for prolonged undifferentiated growth of human embryonic stem cells. Stem Cells 2003;21:546-556.

40. Xu C, Inokuma MS, Denham J et al. Feeder-free growth of undifferentiated human embryonic stem cells. Nat Biotechnol 2001;19:971-974.

41. Braam SR, Zeinstra L, Litjens S et al. Recombinant vitronectin is a functionally defined substrate that supports human embryonic stem cell self-renewal via alphavbeta5 integrin. Stem Cells 2008;26:2257-2265.

42. Miyazaki T, Futaki S, Hasegawa K et al. Recombinant human laminin isoforms can support the undifferentiated growth of human embryonic stem cells. Biochem Biophys Res Commun 2008;375:27-32.

43. Nagaoka M, Si-Tayeb K, Akaike T et al. Culture of human pluripotent stem cells using completely defined conditions on a recombinant E- cadherin substratum. BMC Dev Biol 2010;10:60.

44. Chen G, Gulbranson DR, Hou Z et al. Chemically defined conditions for human iPSC derivation and culture. Nat Methods 2011;8:424-429.

45. Li Y, Powell S, Brunette E et al. Expansion of human embryonic stem cells in defined serum-free medium devoid of animal-derived products. Biotechnol Bioeng 2005;91:688–698.

46. Qian X, Villa-Diaz LG, Krebsbach PH. Advances in culture and manipulation of human pluripotent stem cells. J Dent Res 2013;92:956-962.

47. Villa-Diaz LG, Ross AM, Lahann J et al. Concise review: The evolution of human pluripotent stem cell culture: From feeder cells to synthetic coatings. Stem Cells 2013;31:1-7.

48. Ng HH, Surani MA. The transcriptional and signalling networks of pluripotency. Nat Cell Biol 2011;13:490-496.

49. Jauch R, Ng CK, Saikatendu KS et al. Crystal structure and DNA binding of the homeodomain of the stem cell transcription factor Nanog. J Mol Biol 2008;376:758-770.

50. Nagy A, Vintersten K. Murine embryonic stem cells. Methods Enzymol 2006;418:3-21.

51. Chambers I, Smith A. Self-renewal of teratocarcinoma and embryonic stem cells. Oncogene 2004;23:7150-7160.

52. Rodda DJ, Chew JL, Lim LH et al. Transcriptional regulation of nanog by OCT4 and SOX2. J Biol Chem 2005;280:24731-24737.

53. Chan KK, Zhang J, Chia NY et al. KLF4 and PBX1 directly regulate NANOG expression in human embryonic stem cells. Stem Cells 2009;27:2114-2125.

54. Chen ZY, Wang X, Zhou Y et al. Destabilization of Kruppel-like factor 4 protein in response to serum stimulation involves the ubiquitin-proteasome pathway. Cancer Res 2005;65:10394-10400.

55. Gregory MA, Hann SR. c-Myc proteolysis by the ubiquitin-proteasome pathway: stabilization of c-Myc in Burkitt's lymphoma cells. Mol Cell Biol 2000;20:2423-2435.

56. Moretto-Zita M, Jin H, Shen Z et al. Phosphorylation stabilizes Nanog by promoting its interaction with Pin1. Proc Natl Acad Sci U S A 2010;107:13312-13317.

57. Liao B, Jin Y. Wwp2 mediates Oct4 ubiquitination and its own auto-ubiquitination in a dosage-dependent manner. Cell Res 2010;20:332-344.

58. Xu H, Wang W, Li C et al. WWP2 promotes degradation of transcription factor OCT4 in human embryonic stem cells. Cell Res 2009;19:561-573.

59. Ramakrishna S, Suresh B, Lim KH et al. PEST motif sequence regulating human NANOG for proteasomal degradation. Stem Cells Dev 2011;20:1511-1519.

60. Ebben JD, Zorniak M, Clark PA et al. Introduction to induced pluripotent stem cells: advancing the potential for personalized medicine. World Neurosurg 2011;76:270-275.

61. Plath K, Lowry WE. Progress in understanding reprogramming to the induced pluripotent state. Nat Rev Genet. 2011; 12:253-265.

62. Liao J, Wu Z, Wang Y et al. Enhanced efficiency of generating induced pluripotent stem (iPS) cells from human somatic cells by a combination of six transcription factors. Cell Res 2008;18:600-603.

63. Silva J, Nichols J, Theunissen TW et al. Nanog is the gateway to the pluripotent ground state. Cell 2009;138:722-737.

64 Liu X, Sun H, Qi J et al. Sequential introduction of reprogramming factors reveals a time-sensitive requirement for individual factors and a sequential EMT-MET mechanism for optimal reprogramming. Nat Cell Biol 2013;15:829-838.

FIGURE LEGENDS

Figure 1. Differences in *DPPA5* gene expression and protein levels in human pluripotent stem cells (hPSCs) cultured on irradiated mouse embryonic fibroblasts (MEFs) and feeder-free substrates. (A) Relative transcript levels of *DPPA5* were higher in hESCs (H9) cultured on PMEDSAH compared to on MEFs, while relative transcript levels of *OCT4, SOX2, KLF4, C-MYC* and *NANOG* showed no significant differences in expression. **(B)** Relative transcript levels of *DPPA5* were higher in multiple types of hPSCs (H9, CHB10, hFF-iPSCs, hGF2-iPSCs, and hGF4-iPSCs) cultured on PMEDSAH compared to MEFs. **(C)** Western blot analysis and relative signal intensity of DPPA5, NANOG, OCT4, SOX2, KLF4 and C-MYC proteins in hESCs cultured on MEFs and PMEDSAH. α-tubulin was used as a loading control. **(D)** Compared to when cultured on MEFs, the relative transcript levels of *DPPA5* were higher in hESCs (CHB10) cultured on feeder-free substrates such as

PMEDSAH, Matrigel, Laminin and Vitronectin. Plot data presented as mean ± standard deviation (SD) from three independent experiments (* p<0.05).

Figure 2. Soluble factors and extracellular matrix (ECM) secreted by irradiated mouse embryonic fibroblasts (MEFs) inhibited *DPPA5* expression in human pluripotent stem cells (hPSCs) compared to feeder-free conditions. The control culture condition was PMEDSAH (substrate) plus HCCM (medium). **(A)** Relative transcript levels of *DPPA5* in hESCs cultured in control culture condition, PMEDSAH plus day 1 MEF-conditioned medium (CM), and PMEDSAH plus day 7 MEF-CM. **(B)** Relative transcript levels of *DPPA5* in hESCs cultured in control culture condition, day 1 MEF-ECM plus HCCM, and day 7 MEF-ECM plus HCCM. *OCT4* gene expression was used as a marker indicating the undifferentiated state of the collected hESCs. Data presented as mean ± standard deviation (SD) from three independent experiments, and different letters indicated statistical significance (p<0.05).

Figure 3. Differences in *DPPA5* expression between undifferentiated and differentiated human pluripotent stem cells (hPSCs), and somatic cells. (A) Relative transcript levels of *DPPA5* increased in iPSCs (hFF-iPSCs, hGF2-iPSCs and hGF4-iPSCs) compared to corresponding parental fibroblasts. **(B)** Relative transcript levels of *OCT4*, *SOX2* and *DPPA5* decreased after embryoid body formation from hESCs. **(C)** Relative transcript levels of *DPPA5* decreased after directed cell lineage differentiation from hESCs into endodermal, mesodermal and ectodermal derivatives.

Data presented as mean ± standard deviation (SD) from three independent experiments (* p<0.05).

Figure 4. Regulation of NANOG protein levels by DPPA5 in human pluripotent stem cells (hPSCs). (A) Relative transcript levels of *DPPA5, NANOG, OCT4, SOX2, KLF4 and C-MYC* between control fibroblasts and with *DPPA5* overexpression. **(B)** Western blot analysis and relative signal intensity of DPPA5, NANOG, OCT4, SOX2, KLF4 and C-MYC proteins between control fibroblasts and fibroblasts with *DPPA5* overexpression. β-actin was used as a loading control. **(C)** Relative transcript levels of *DPPA5, NANOG, OCT4, SOX2, KLF4 and C-MYC* between control hESCs and hESCs with *DPPA5* overexpression. **(D)** Western blot analysis and relative signal intensity of DPPA5, NANOG, OCT4, SOX2, KLF4 and C-MYC proteins between control hESCs and hESCs with *DPPA5* overexpression. β-actin was used as a loading control. Plot data is presented as mean ± standard deviation (SD) from three independent experiments (* p<0.05).

Figure 5. Protein interaction and stabilization between DPPA5 and NANOG in human pluripotent stem cells (hPSCs). (A) Representative confocal microscopy images of immune fluorescent staining of hESCs with NANOG and DPPA5 primary antibodies. 4', 6-diamidino-2-phenylindole (DAPI) shows nuclear staining. The merged images indicate the co-localization of DPPA5 and NANOG in hESC nucleus. Scale bars, 5 μm. **(B)** Co-immunoprecipitation of endogenous NANOG and DPPA5 in

hESCs. hESCs extracts prepared in CHAPS lysis and IP buffer were immunoprecipitated with anti-NANOG or control IgG antibody. The immune complexes and the input (whole hESC lysate) were analyzed by Western blot with antibodies specific to NANOG or DPPA5. **(C)** Co-immunoprecipitation of DDK-DPPA5 and NANOG in hESCs. hESCs were transfected with DDK-tagged DPPA5 plasmid. hESCs extracts prepared in CHAPS lysis and IP buffer were immunoprecipitated with anti-DDK or control IgG antibody. The immune complexes and the input (whole hESC lysate) were analyzed by Western blot with antibodies specific to DDK and NANOG. **(D)** The protein levels of NANOG and DPPA5 in control hESCs or hESCs with *DPPA5* overexpression were analyzed at the indicated time points after cycloheximide (CHX; 45 μg/ml) treatment. Western blot analysis and relative signal intensity indicated that DPPA5 supports NANOG protein stability in hESCs. β-actin was used as a loading control. Plot data is presented as mean ± standard deviation (SD) from three independent experiments (* $p<0.05$).

Figure 6. DPPA5 enhances the function of NANOG in human pluripotent stem cells (hPSCs). (A) The expression of NANOG target genes regulated by DPPA5. Relative transcript level of *SALL4* was higher, while *GATA6* and *SOCS3* were lower in hESCs with *DPPA5* overexpression compared to the control hESCs. **(B)** hESC differentiation regulated by DPPA5. After induced neuroectoderm differentiation in hESCs, the expression levels of pluripotency markers such as *OCT4* and *SOX2* decreased, while neuroectordern markers *SOX1* and *NEUROD1* increased in both

control and DPPA5 overexpressed cells. In neuroectoderm differentiated cells, the expression levels of *SOX1* and *NEUROD1* were lower in DPPA5 overexpressed cells compared to controls. Data presented as mean ± standard deviation (SD) from three independent experiments (* $p<0.05$).

Figure 7. DPPA5 overexpression has an additive effect in human induced pluripotent stem cell (hiPSC)-reprogramming. Day 6, day 9 and day 12-DPPA5 added groups (d6+D, d9+D, d12+D) had higher iPSC colony number compared to control group and day 0-DPPA5 added group (d0+D). In control group (Con), fibroblasts were infected on day 0 with retroviruses encoding *KLF4, C-MYC, OCT4* and *SOX2*, *(KMOS)* while in experimental groups in addition to this cocktail of reprogramming factors, cells were also infected with retrovirus encoding *DPPA5* on day 0 (d0+D), day 6 (d6+D), day 9 (d9+D) and day 12 (d12+D). hiPSC colonies were identified by positive alkaline phosphatase (ALP) staining and morphological characteristics of colonies, quantified and compared among groups. Plot data is presented as mean ± standard deviation (SD) from three independent experiments (* $p<0.05$).

Paul Krebsbach Top

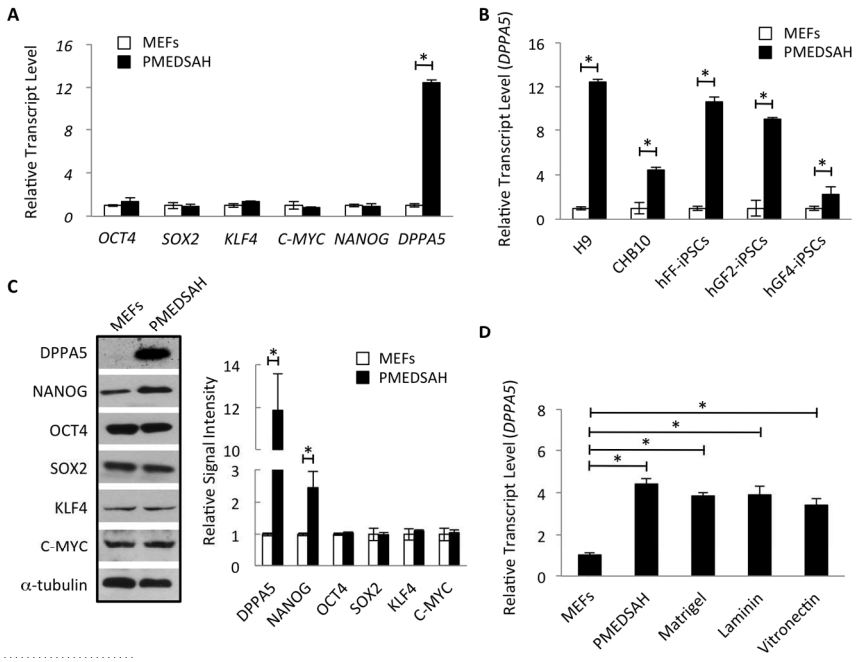

Fig. 1

Figure 1. Differences in DPPA5 gene expression and protein levels in human pluripotent stem cells (hPSCs) cultured on irradiated mouse embryonic fibroblasts (MEFs) and feeder-free substrates. (A) Relative transcript levels of DPPA5 were higher in hESCs (H9) cultured on PMEDSAH compared to on MEFs, while relative transcript levels of OCT4, SOX2, KLF4, C-MYC and NANOG showed no significant differences in expression. (B) Relative transcript levels of DPPA5 were higher in multiple types of hPSCs (H9, CHB10, hFF-iPSCs, hGF2-iPSCs, and hGF4-iPSCs) cultured on PMEDSAH compared to MEFs. (C) Western blot analysis and relative signal intensity of DPPA5, NANOG, OCT4, SOX2, KLF4 and C-MYC proteins in hESCs cultured on MEFs and PMEDSAH. α-tubulin was used as a loading control. (D) Compared to when cultured on MEFs, the relative transcript levels of DPPA5 were higher in hESCs (CHB10) cultured on feeder-free substrates such as PMEDSAH, Matrigel, Laminin and Vitronectin. Plot data presented as mean ± standard deviation (SD) from three independent experiments (* $p<0.05$).
595x793mm (72 x 72 DPI)

Paul Krebsbach Top

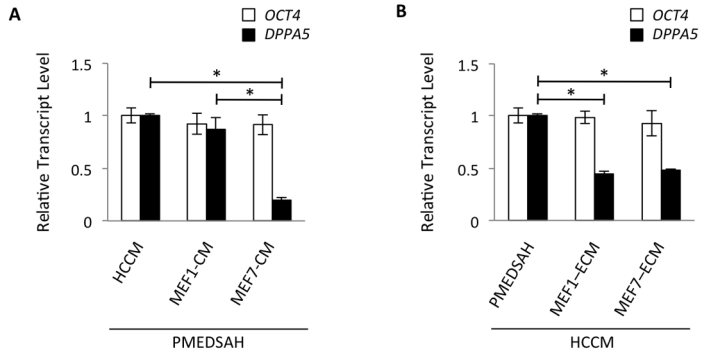

Fig. 2

Figure 2. Soluble factors and extracellular matrix (ECM) secreted by irradiated mouse embryonic fibroblasts (MEFs) inhibited DPPA5 expression in human pluripotent stem cells (hPSCs) compared to feeder-free conditions. The control culture condition was PMEDSAH (substrate) plus HCCM (medium). (A) Relative transcript levels of DPPA5 in hESCs cultured in control culture condition, PMEDSAH plus day 1 MEF-conditioned medium (CM), and PMEDSAH plus day 7 MEF-CM. (B) Relative transcript levels of DPPA5 in hESCs cultured in control culture condition, day 1 MEF-ECM plus HCCM, and day 7 MEF-ECM plus HCCM. OCT4 gene expression was used as a marker indicating the undifferentiated state of the collected hESCs. Data presented as mean ± standard deviation (SD) from three independent experiments, and different letters indicated statistical significance ($p<0.05$).
595x793mm (72 x 72 DPI)

Paul Krebsbach Top

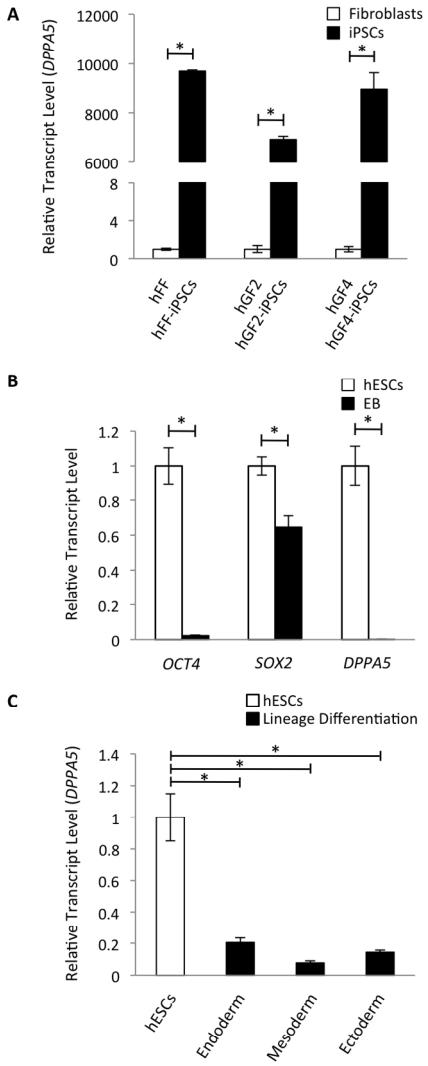

Fig. 3

Figure 3. Differences in DPPA5 expression between undifferentiated and differentiated human pluripotent stem cells (hPSCs), and somatic cells. (A) Relative transcript levels of DPPA5 increased in iPSCs (hFF-iPSCs, hGF2-iPSCs and hGF4-iPSCs) compared to corresponding parental fibroblasts. (B) Relative transcript levels of OCT4, SOX2 and DPPA5 decreased after embryoid body formation from hESCs. (C) Relative transcript levels of DPPA5 decreased after directed cell lineage differentiation from hESCs into endodermal, mesodermal and ectodermal derivatives. Data presented as mean ± standard deviation (SD) from three independent experiments (* $p<0.05$).
595x793mm (72 x 72 DPI)

Paul Krebsbach Top

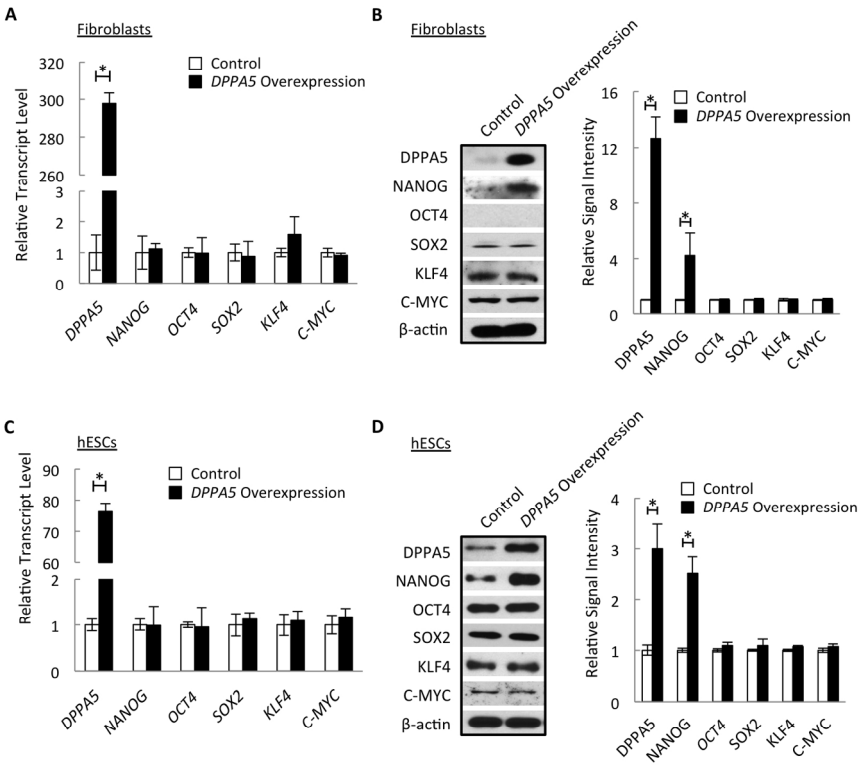

Fig. 4

Figure 4. Regulation of NANOG protein levels by DPPA5 in human pluripotent stem cells (hPSCs). (A) Relative transcript levels of DPPA5, NANOG, OCT4, SOX2, KLF4 and C-MYC between control fibroblasts and with DPPA5 overexpression. (B) Western blot analysis and relative signal intensity of DPPA5, NANOG, OCT4, SOX2, KLF4 and C-MYC proteins between control fibroblasts and fibroblasts with DPPA5 overexpression. β-actin was used as a loading control. (C) Relative transcript levels of DPPA5, NANOG, OCT4, SOX2, KLF4 and C-MYC between control hESCs and hESCs with DPPA5 overexpression. (D) Western blot analysis and relative signal intensity of DPPA5, NANOG, OCT4, SOX2, KLF4 and C-MYC proteins between control hESCs and hESCs with DPPA5 overexpression. β-actin was used as a loading control. Plot data is presented as mean ± standard deviation (SD) from three independent experiments (* $p<0.05$).
595x793mm (72 x 72 DPI)

Paul Krebsbach Top

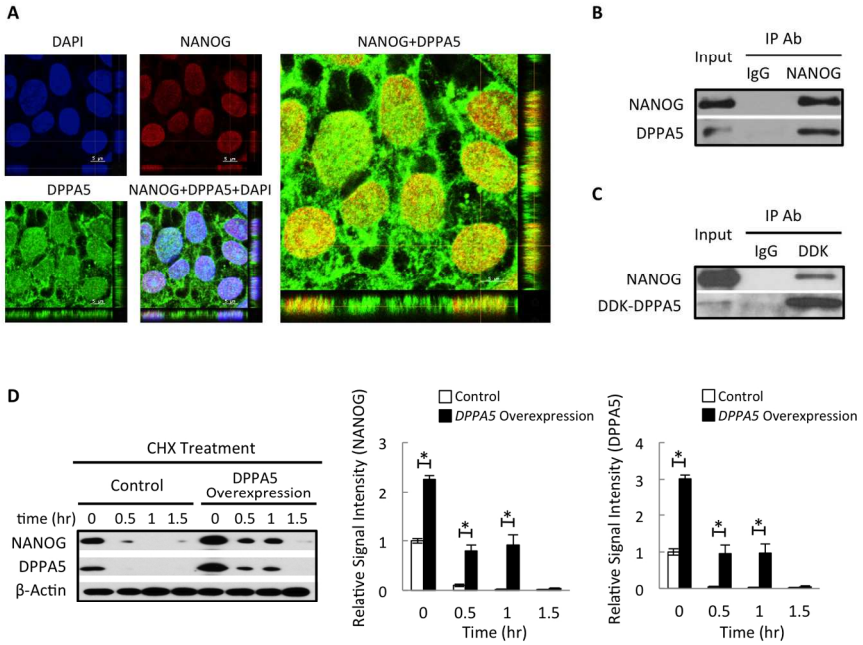

Fig. 5

Figure 5. Protein interaction and stabilization between DPPA5 and NANOG in human pluripotent stem cells (hPSCs). (A) Representative confocal microscopy images of immune fluorescent staining of hESCs with NANOG and DPPA5 primary antibodies. 4', 6-diamidino-2-phenylindole (DAPI) shows nuclear staining. The merged images indicate the co-localization of DPPA5 and NANOG in hESC nucleus. Scale bars, 5 μm. (B) Co-immunoprecipitation of endogenous NANOG and DPPA5 in hESCs. hESCs extracts prepared in CHAPS lysis and IP buffer were immunoprecipitated with anti-NANOG or control IgG antibody. The immune complexes and the input (whole hESC lysate) were analyzed by Western blot with antibodies specific to NANOG or DPPA5. (C) Co-immunoprecipitation of DDK-DPPA5 and NANOG in hESCs. hESCs were transfected with DDK-tagged DPPA5 plasmid. hESCs extracts prepared in CHAPS lysis and IP buffer were immunoprecipitated with anti-DDK or control IgG antibody. The immune complexes and the input (whole hESC lysate) were analyzed by Western blot with antibodies specific to DDK and NANOG. (D) The protein levels of NANOG and DPPA5 in control hESCs or hESCs with DPPA5 overexpression were analyzed at the indicated time points after cycloheximide (CHX; 45 μg/ml) treatment. Western blot analysis and relative signal intensity indicated that

DPPA5 supports NANOG protein stability in hESCs. β-actin was used as a loading control. Plot data is presented as mean ± standard deviation (SD) from three independent experiments (* $p<0.05$).
595x793mm (72 x 72 DPI)

Paul Krebsbach Top

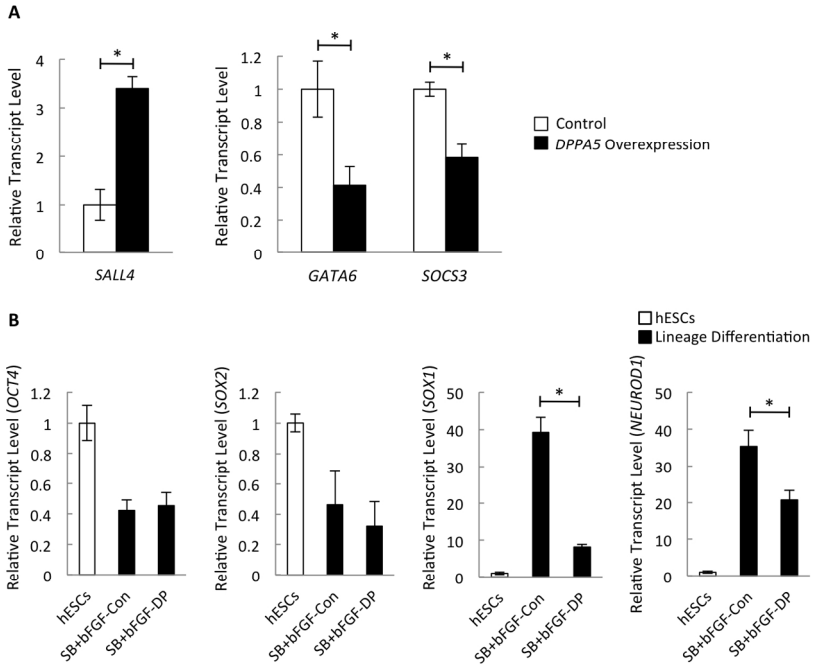

Fig. 6

Figure 6. DPPA5 enhances the function of NANOG in human pluripotent stem cells (hPSCs). (A) The expression of NANOG target genes regulated by DPPA5. Relative transcript level of SALL4 was higher, while GATA6 and SOCS3 were lower in hESCs with DPPA5 overexpression compared to the control hESCs. (B) hESC differentiation regulated by DPPA5. After induced neuroectoderm differentiation in hESCs, the expression levels of pluripotency markers such as OCT4 and SOX2 decreased, while neuroectordern markers SOX1 and NEUROD1 increased in both control and DPPA5 overexpressed cells. In neuroectoderm differentiated cells, the expression levels of SOX1 and NEUROD1 were lower in DPPA5 overexpressed cells compared to controls. Data presented as mean ± standard deviation (SD) from three independent experiments (* $p<0.05$).
595x793mm (72 x 72 DPI)

Paul Krebsbach Top

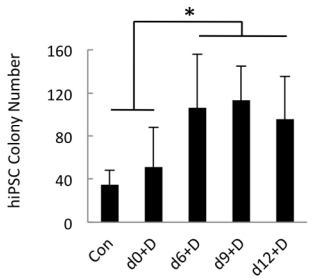

Fig. 7

Figure 7. DPPA5 overexpression has an additive effect in human induced pluripotent stem cell (hiPSC)-reprogramming. Day 6, day 9 and day 12-DPPA5 added groups (d6+D, d9+D, d12+D) had higher iPSC colony number compared to control group and day 0-DPPA5 added group (d0+D). In control group (Con), fibroblasts were infected on day 0 with retroviruses encoding KLF4, C-MYC, OCT4 and SOX2, (KMOS) while in experimental groups in addition to this cocktail of reprogramming factors, cells were also infected with retrovirus encoding DPPA5 on day 0 (d0+D), day 6 (d6+D), day 9 (d9+D) and day 12 (d12+D). hiPSC colonies were identified by positive alkaline phosphatase (ALP) staining and morphological characteristics of colonies, quantified and compared among groups. Plot data is presented as mean ± standard deviation (SD) from three independent experiments (* $p<0.05$).
595x793mm (72 x 72 DPI)

Supplemental Information - Krebsbach et al.

Supplemental Figure 1. Induced specific lineage differentiation from human embryonic stem cells (hESCs) with expression of genes representing different germ layers. hESCs were induced to endodermal, mesodermal and ectodermal lineages. Cell lineage differentiation was confirmed by quantitative RT-PCR using the probe of factors representative of each germ layer. Data were presented as mean ± SD from three independent experiments (* $p<0.05$).

Supplemental Figure 2. DPPA5 expression decreased in differentiated human pluripotent stem cells (hPSCs). (A) Representative micrographs showing expression of DPPA5 in undifferentiated hESCs. NANOG was used as to verify the undifferentiated state of cells. **(B)** Representative micrographs showing the reduced expression of DPPA5 in differentiated hESCs (ectoderm differentiation). NANOG was used as to verify the undifferentiated state of cells. **(C)** Co-immunoprecipitation of endogenous OCT4 and DPPA5 in hESCs. hESCs extracts prepared in CHAPS lysis and IP buffer were immunoprecipitated with anti-OCT4 or control IgG antibody. The immune complexes and the input (whole hESC lysate) were analyzed by Western blot with antibodies specific to OCT4 or DPPA5. **(D)** Co-immunoprecipitation of endogenous SOX2 and DPPA5 in hESCs. hESCs extracts prepared in CHAPS lysis and IP buffer were immunoprecipitated with anti-SOX2 or control IgG antibody. The immune complexes and the input (whole hESC lysate) were analyzed by Western

blot with antibodies specific to SOX2 or DPPA5.

Supplemental Figure 3. DPPA5 support reprogramming of fibroblasts into human induced pluripotent stem cells (hiPSCs). Representative bright-field images of **(A)** parental fibroblasts and **(B)** corresponding fully reprogrammed hiPSCs. Scale bars, 100 μm. **(C)** Representative bright-field image of a hiPSC colony classified as reprogrammed by alkaline phosphatase positive staining and well-defined borders. Scale bars, 500 μm. **(D)** Representative bright-field image of a colony classified as pre-iPSCs, because its borders are not well-defined despite expressing alkaline phosphatase activity. Representative immunofluorescent micrographs showing expression of pluripotency markers OCT4, SOX2, NANOG, TRA-1-81, TRA-1-60, SSEA4 and SSEA3 in hiPSCs reprogrammed by **(E)** overexpression of KLF4, C-MYC, OCT4 and SOX2, and **(F)** with the addition of DPPA5. Scale bars, 100 μm.

Supplemental Figure 4. Additive effect of DPPA5 in hiPSC reprogramming. Reprogramming of fibroblasts into hiPSCs was performed using irradiated-mouse embryonic fibroblasts (MEF) or Matrigel coated plates as substrates. At day 23 post infection, flow cytometry analysis was done to quantify the expression of pluripotent stem cell markers TRA-1-60 and SSEA4 in control group (cells infected only with *KLF4, C-MYC, OCT4 and SOX2 (KMOS)*) versus d6+D group (cell infected with *KMOS* plus *DPPA5* at day 6). Plot data is presented as mean ± standard deviation

(SD) from three independent experiments (* $p<0.05$).

Supplemental Table 1. Embryoid body (EB) formation from hESCs with expression of genes representing different germ layers

Supplemental Table 2. DPPA5 increased human induced pluripotent stem cell (hiPSC)-reprogramming efficiency.

Supplemental Table 3. Embryoid body (EB) formation from control hiPSCs with expression of genes representing different germ layers

Supplemental Table 4. Embryoid body (EB) formation from d6+D-hiPSCs with expression of genes representing different germ layers

Paul Krebsbach Top

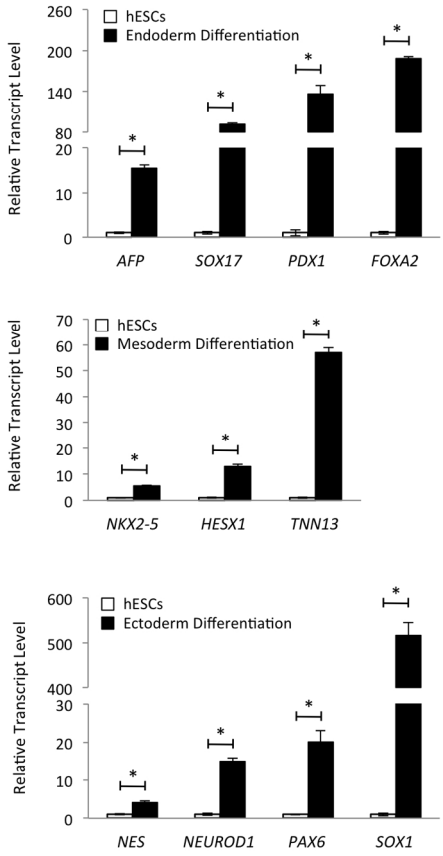

Supplemental Fig. 1

Supplemental Figure 1. Induced specific lineage differentiation from human embryonic stem cells (hESCs) with expression of genes representing different germ layers. hESCs were induced to endodermal, mesodermal and ectodermal lineages. Cell lineage differentiation was confirmed by quantitative RT-PCR using the probe of factors representative of each germ layer. Data were presented as mean ± SD from three independent experiments (* $p<0.05$).
595x793mm (72 x 72 DPI)

Paul Krebsbach Top

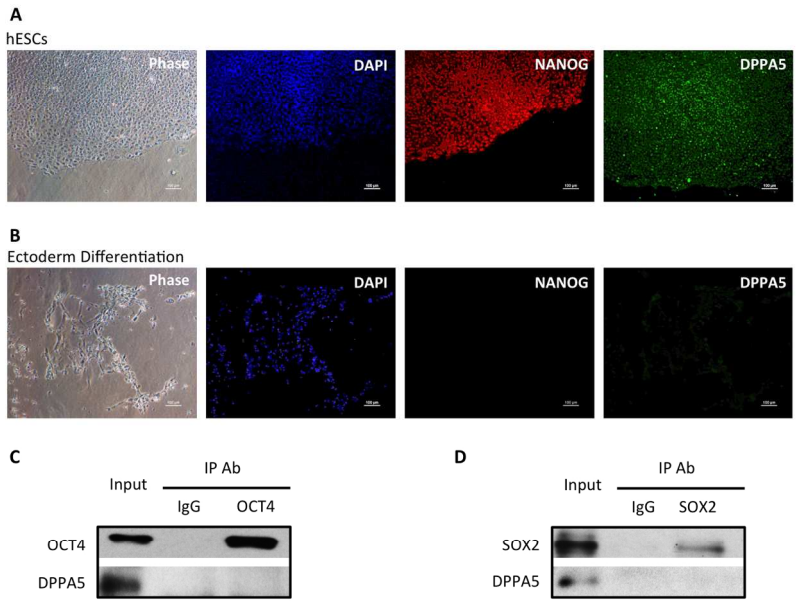

Supplemental Fig. 2

Supplemental Figure 2. DPPA5 expression decreased in differentiated human pluripotent stem cells (hPSCs). (A) Representative micrographs showing expression of DPPA5 in undifferentiated hESCs. NANOG was used as to verify the undifferentiated state of cells. (B) Representative micrographs showing the reduced expression of DPPA5 in differentiated hESCs (ectoderm differentiation). NANOG was used as to verify the undifferentiated state of cells. (C) Co-immunoprecipitation of endogenous OCT4 and DPPA5 in hESCs. hESCs extracts prepared in CHAPS lysis and IP buffer were immunoprecipitated with anti-OCT4 or control IgG antibody. The immune complexes and the input (whole hESC lysate) were analyzed by Western blot with antibodies specific to OCT4 or DPPA5. (D) Co-immunoprecipitation of endogenous SOX2 and DPPA5 in hESCs. hESCs extracts prepared in CHAPS lysis and IP buffer were immunoprecipitated with anti-SOX2 or control IgG antibody. The immune complexes and the input (whole hESC lysate) were analyzed by Western blot with antibodies specific to SOX2 or DPPA5.
595x793mm (72 x 72 DPI)

Paul Krebsbach Top

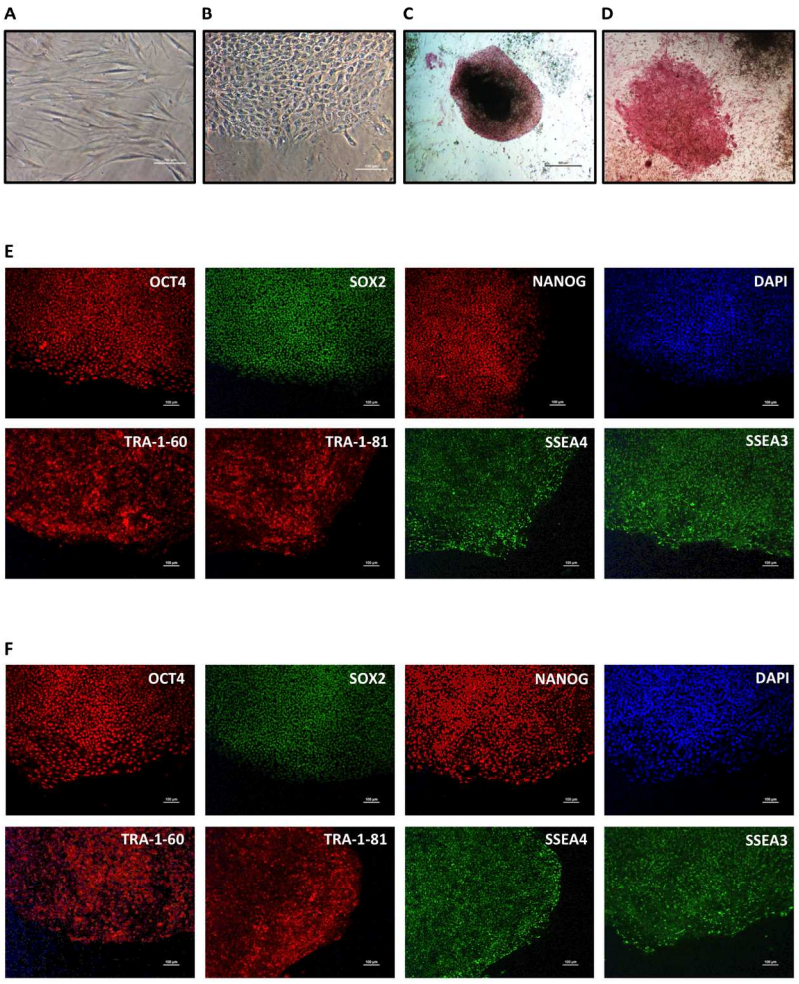

Supplemental Fig. 3

Supplemental Figure 3. DPPA5 support reprogramming of fibroblasts into human induced pluripotent stem cells (hiPSCs). Representative bright-field images of (A) parental fibroblasts and (B) corresponding fully reprogrammed hiPSCs. Scale bars, 100 μm. (C) Representative bright-field image of a hiPSC colony classified as reprogrammed by alkaline phosphatase positive staining and well-defined borders. Scale bars, 500 μm. (D) Representative bright-field image of a colony classified as pre-iPSCs, because its borders are not well-defined despite expressing alkaline phosphatase activity. Representative immunofluorescent micrographs showing expression of pluripotency markers OCT4, SOX2, NANOG, TRA-1-81, TRA-1-60, SSEA4 and SSEA3 in hiPSCs reprogrammed by (E) overexpression of KLF4, C-MYC, OCT4 and SOX2, and (F) with the addition of DPPA5. Scale bars, 100 μm.
595x793mm (72 x 72 DPI)

Paul Krebsbach Top

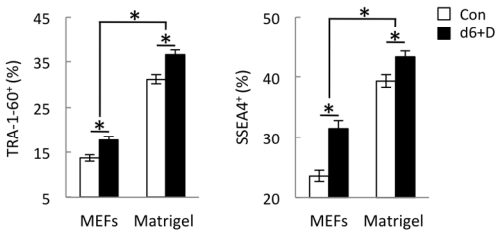

Supplemental Fig. 4

Supplemental Figure 4. Additive effect of DPPA5 in hiPSC reprogramming. Reprogramming of fibroblasts into hiPSCs was performed using irradiated-mouse embryonic fibroblasts (MEF) or Matrigel coated plates as substrates. At day 23 post infection, flow cytometry analysis was done to quantify the expression of pluripotent stem cell markers TRA-1-60 and SSEA4 in control group (cells infected only with KLF4, C-MYC, OCT4 and SOX2 (KMOS)) versus d6+D group (cell infected with KMOS plus DPPA5 at day 6). Plot data is presented as mean ± standard deviation (SD) from three independent experiments (* $p<0.05$).
595x793mm (72 x 72 DPI)

Supplemental Table 1. Embryoid body (EB) formation from hESCs with expression of genes representing different germ layers

	Gene	Relative Transcript Level ± SD
Endoderm	*PDX1*	28.24 ± 3.70
	AFP	42.18 ± 4.39
	SOX17	126.57 ± 6.58
	FOXA2	237.87 ± 20.9
Mesoderm	*HESX1*	11.2 ± 1.88
	TNN13	110.88 ± 2.28
	NKX2-5	122.86 ± 17.48
Ectoderm	*NES*	3.84 ± 0.67
	SOX1	34.76 ± 1.98
	PAX6	89.24 ± 3.03
	NEUROD1	683.19 ± 89.38

Supplemental Table 2. DPPA5 increased human induced pluripotent stem cell (hiPSC)-reprogramming efficiency.

	hiPSC Colony Number ± SD	Reprogramming Efficiency (%)
Con	34.6 ± 13.5	0.023
d0+D	51.3 ± 36.6	0.034
d6+D	106.6 ± 49	0.071
d9+D	113.6 ± 31.4	0.076
d12+D	96.3 ± 39.2	0.064

Supplemental Table 3. Embryoid body (EB) formation from control hiPSCs with expression of genes representing different germ layers

	Gene	Relative Transcript Level ± SD
Endoderm	*SOX17*	4.97 ± 0.23
	FOXA2	10.50 ± 1.11
	AFP	625.62 ± 20.32
Mesoderm	*T*	1.67 ± 0.35
	HESX1	3.42 ± 0.13
	NKX2-5	33.26 ± 1.14
Ectoderm	*NEUROD1*	3.12 ± 0.13
	SOX1	4.57 ± 0.17
	PAX6	9.93 ± 0.47

Supplemental Table 4. Embryoid body (EB) formation from d6+D-hiPSCs with expression of genes representing different germ layers

	Gene	Relative Transcript Level ± SD
Endoderm	*SOX17*	5.07 ± 0.30
	FOXA2	4.80 ± 0.29
	AFP	878.20 ± 54.71
Mesoderm	*T*	1.45 ± 0.27
	HESX1	4.45 ± 0.14
	NKX2-5	29.31 ± 7.51
Ectoderm	*NEUROD1*	7.77 ± 0.08
	SOX1	7.99 ± 0.31
	PAX6	18.84 ± 2.43